K. Rokosz[1a], T. Hryniewicz[1], F. Simon[2b], S. Rzadkiewicz[1]

[1] *Koszalin University of Technology, Faculty of Mechanical Engineering, Division of Surface Electrochemistry, Racławicka 15-17, 75-620 Koszalin, Poland*
[2]*Department of Polymer Interfaces, Leibniz Institute of Polymer Research Dresden, Hohe Strasse 6, D-01069 Dresden, Germany*
[a] *rokosz@tu.koszalin.pl,* [b]*frsimon@ipfdd.de*

XPS ANALYSIS OF AISI 304L STAINLESS STEEL SURFACE AFTER ELECTROPOLISHING

ABSTRACT

In the paper, the passive surface layers of AISI 304L after standard (EP50) and very-high-current density electropolishing (EP1000) in a mixture of orthophosphoric and sulfuric acids in a 1:4 ratio, are presented. The main finding of the presented studies is enrichment of the steel surface film in chromium: total chromium to total iron ratio was equal to 6.6 after EP50 and to 2.8 after EP1000; on the other hand, chromium compounds to iron compounds ratio was equal to 10.1 after EP50, and 3.9 after EP1000.

Keywords: Electropolishing, XPS; AISI 304L SS; Cr/Fe ratio

INTRODUCTION

Austenitic stainless steels after electropolishing can be used in food and chemical industries as well as in medicine (biomaterial) because of their chemical composition. The standard electropolishing [1-2] as well as magnetoelectropolishing [2-12] of stainless steels can change the chemical composition of passive layers formed after these electrochemical treatments [1-7]. These electrochemical polishing treatments can also have an impact on improvement of the corrosion resistance [8-9], roughness and shine [10, 11, 13]. In the presented paper Authors show one part of the experiment plan, with the electrolyte consisting of 20 vol% H_3PO_4 and 80 vol% H_2SO_4. The whole plan covers four electrolytes based on the phosphoric and sulfuric acids, *i.e.* 1:4; 2:3; 3:2; 4:1, including the studies with two current densities 50 A/dm^2 and 1000 A/dm^2, respectively.

EXPERIMENTAL

The AISI 304L stainless steel samples were used for the study, with the material composition presented in Table 1. The samples were cut off from a cold-rolled metal sheet of the stainless steel after plate rolling so that the austenitic structure was retained. They were prepared in the form of rectangular specimens of dimensions 30×5 mm cut of the metal sheet 1 mm thick.

Table 1. Chemical composition of AISI 304L SS (wt%)

C	Cr	Ni	Mn	Mo	P	S	Cu
0.04	18.1	8.15	1.25	0.22	0.029	0.004	0.29
Si	**Co**	**B**	**Al**	**Sn**	**N$_2$**	**V**	**Fe**
0.44	0.17	0.002	0.002	0.007	0.078	0.09	bal.

The electrolytic polishing operations were performed at the current density of 1000±10 A/dm^2. The main elements of set-up were: a processing cell, a direct current (DC) power supply RNG-3010, the electrodes and connecting wiring. The studies were carried out in the electrolyte of initial temperature of 40±2 °C. For the studies, as an electrolyte a mixture of orthophosphoric and sulfuric acids 1:4, was used. The electrolytic cell was used, containing up to 500 cm^3 of the electrolyte solution. Additional steels samples treated by a standard electropolishing EP at the current density of 50±1 A/dm^2 were used for a reference; they were prepared in the same solution as the previous treatments in temperature of 65±5 °C. Before the samples were measured, they were rinsed with ethanol.

All the X-ray photoelectron spectroscopy (XPS) studies were carried out by means of an Axis Ultra photoelectron spectrometer (Kratos Analytical, Manchester, UK). The spectrometer was equipped with a monochromatic Al Kα ($h \cdot v$ = 1486.6 eV) X-ray source of 300 W at 15 kV. The kinetic energy of photoelectrons was determined with a hemispheric analyzer set to pass energy of 160 eV for the wide-scan spectra and 20 eV for high-resolution spectra. During all measurements, electrostatic charging of the sample was avoided by means of a low-energy electron source working in combination with a magnetic immersion lens. Later, all recorded peaks were shifted by the same value that was necessary to set the C 1s peak to 284.8 eV. For measurements the take-off angle, here defined as an angle between the sample surface normal and the electron-optical axis of the spectrometer, was 0°. Hence, the maximum information depth of the XPS method was not more than 10 nm. The quantitative elemental compositions were determined from the peak areas using experimentally determined sensitivity factors and the spectrometer transmission function. The spectrum background was subtracted according to Shirley [14, 15]. The high-resolution spectra were deconvoluted by CasaXPS software [16-18].

RESULTS

The S 2p spectra after standard EP50 and after high-current density EP1000 electropolishings are shown in Fig. 1. The binding energy of the detected peaks indicates the iron and/or chromium sulphates. In the case of phosphorus P 2p spectra the most probable interpretation of the peaks is iron and/or chromium phosphates, that is displayed in Figure 2. The Ni 2p, Cr 2p and Fe 2p spectra are visible in Fig. 3-5.
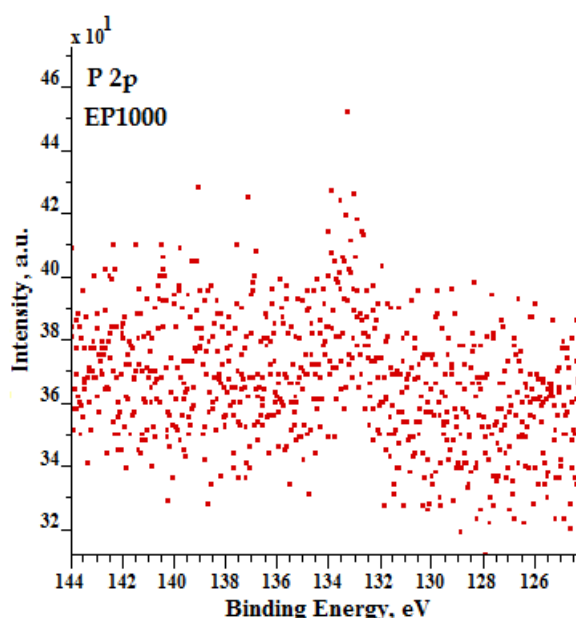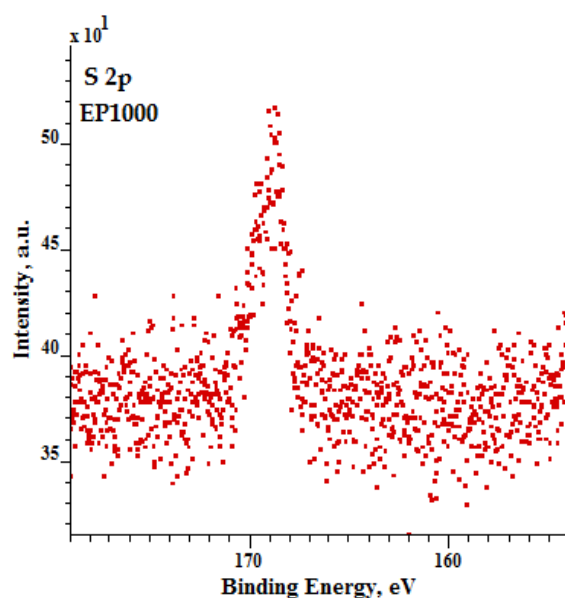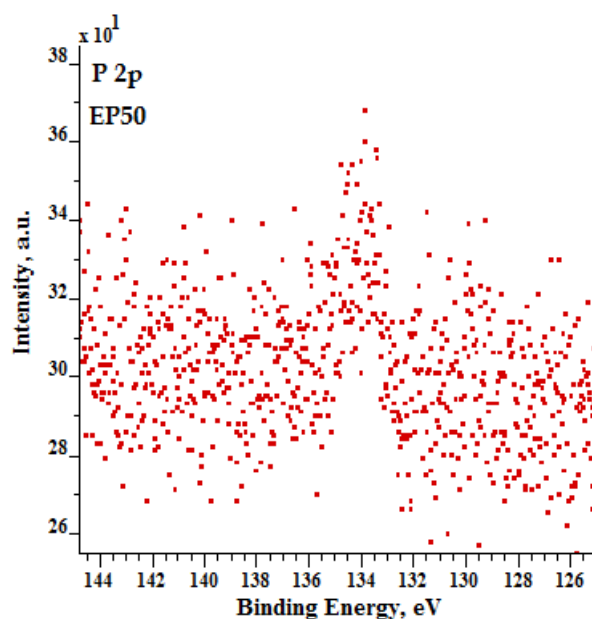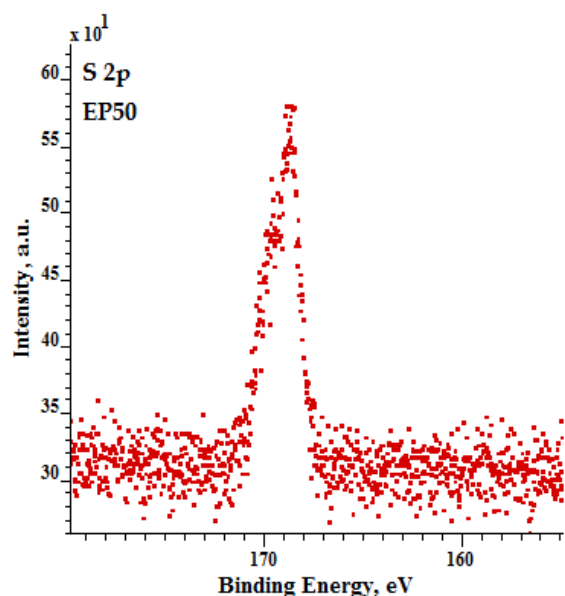

Fig. 1. XPS high-resolution of S 2p spectra of AISI 304L surface layer after EP50 and EP1000, respectively

Fig. 2. XPS high-resolution of P 2p spectra of AISI 304L surface layer after EP50 and EP1000, respectively
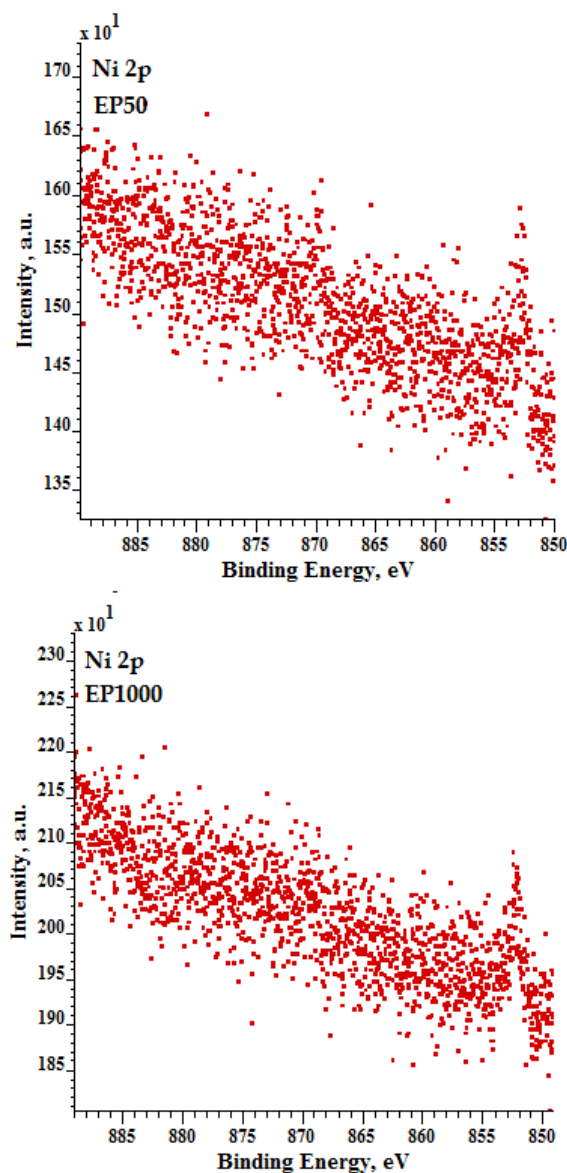
Fig. 3. XPS high-resolution of Ni 2p spectra of AISI 304L surface layer after EP50 and EP1000, respectively

In Tables 2 and 3, the XPS high-resolution of Cr 2p spectra of AISI 304L surface layer after EP50 and EP1000, are presented. After a standard EP50 electropolishing in the surface layer down to about 10 nm here over two times more metallic chromium (Cr^0) than after high-current density electropolishing EP1000, was detected. In the case of chromium on the third (Cr^{3+}) and sixth (Cr^{6+}) oxidation stages the higher amount is noted after EP1000. It is most likely that the chromium on the third oxidation stage occurs as Cr_2O_3, $CrOOH$, $Cr_2(SO_4)_3$, $CrPO_4$. In Tables 4 and 5, the XPS high-resolution of Fe 2p spectra of AISI 304L surface layer after EP50 and EP1000, are presented. After EP50 there is more iron as a metal (Fe^0) and less iron (Fe^{2+} and Fe^{3+}) compounds (oxides: FeO, Fe_2O_3, Fe_3O_4; hydroxide: $FeOOH$; sulphates: $FeSO_4$, $Fe_2(SO_4)_3$ and phosphates: $Fe_3(PO_4)_2$, $FePO_4$), than those after EP1000.
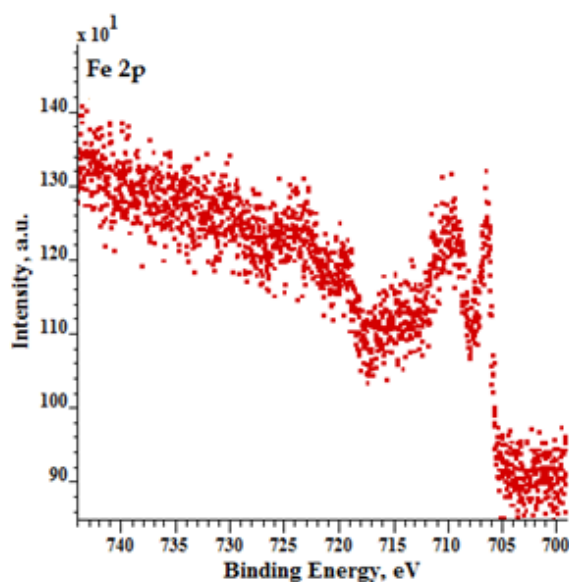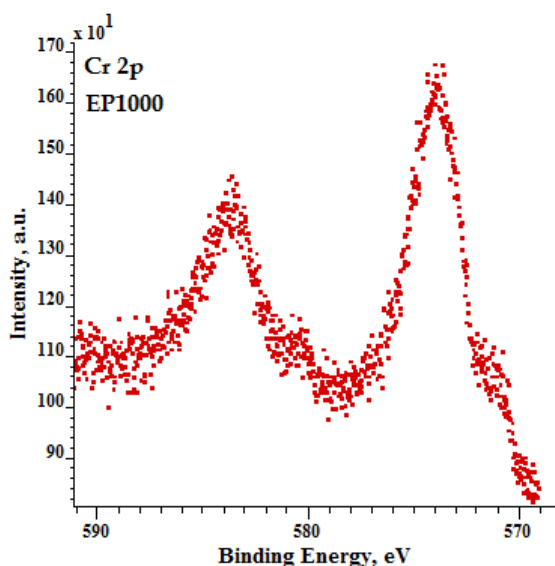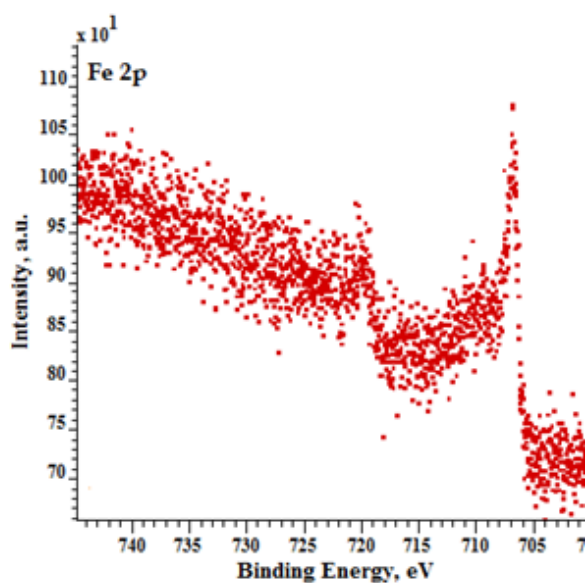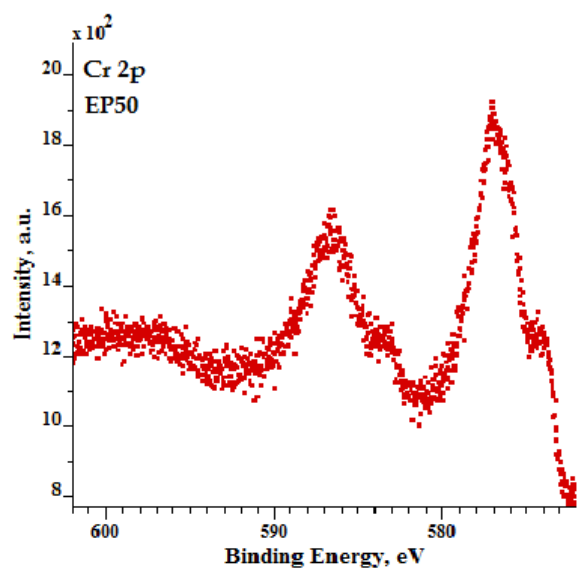
Fig. 4. XPS high-resolution of Cr 2p spectra of AISI 304L surface layer after EP50 and EP1000, respectively

Fig. 5. XPS high-resolution of Fe 2p spectra of AISI 304L surface layer after EP50 and EP1000, respectively

Table 2. Results of fitting Cr 2p$_{3/2}$ of EP50 and EP1000 data

	EP50			**EP1000**		
BE [eV]	574.1	576.9	579.5	574.1	576.9	579.5
FWHM	1.3	2.6	1.8	1.1	2.6	2.8
Cr 2p [at%]	28.7	67.1	4.2	12.1	81.8	6.1
Line shape	LA(1.3,4,5)	GL(30)	GL(30)	LA(1.3,4,5)	GL(30)	GL(30)
Cr^x	**Cr^0**	**Cr^{3+}**	**Cr^{6+}**	**Cr^0**	**Cr^{3+}**	**Cr^{6+}**

Table 3. XPS high-resolution of Cr 2p spectra of AISI 304L surface layer after EP50 and EP1000
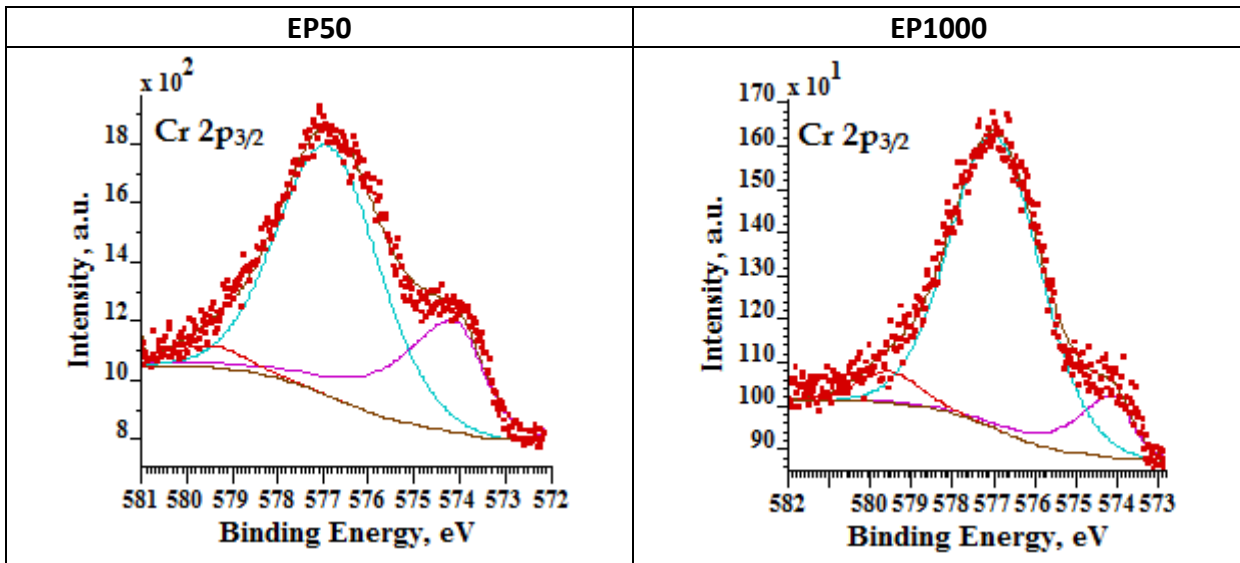
EP50	EP1000

Table 4. *Results of fitting Fe 2p$_{3/2}$ of EP50 and EP1000 data*

	EP50		EP1000	
BE [eV]	706.6	709.6	706.6	710.0
FWHM	0.7	4.8	0.7	3.6
Fe 2p [at%]	53.5	46.5	37.8	62.2
Line shape	LA(1.2,4.8,3)	GL(30)	LA(1.2,4.8,3)	GL(30)
Fe^x	**Fe^0**	**Fe^{2+}, Fe^{3+}**	**Fe^0**	**Fe^{2+}, Fe^{3+}**

Table 5. *XPS high-resolution of Fe 2p spectra of AISI 304L surface layer after EP50 and EP1000*

EP50	EP1000
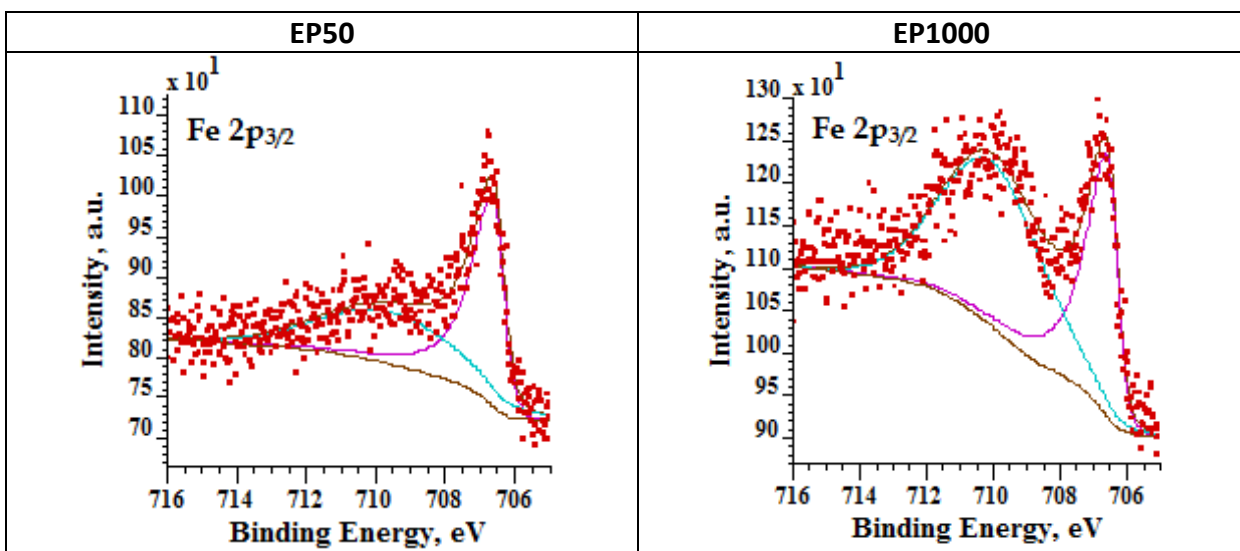
In Figure 6, there are presented the chromium metal to iron metal (Cr-M/Fe-M), chromium compounds to iron compounds (Cr-X/Fe-X) and total chromium to total iron (Cr/Fe) ratios on the basis of the high-resolution XPS spectra. For all ratios the higher column is visible after the standard EP50 electropolishing. Authors obtained here very high total Cr/Fe and compounds Cr-X/Fe-X ratios, which after EP50 were equal to 6.6 and 10.1, respectively. The finding is very important in the case of corrosion resistance as well as biocompatibility. In the case of a lower amount of total chromium the general corrosion can be a little bit higher, but it will be studied by Authors soon. On the other hand, a smaller amount of chromium in the outer passive layer, that comes in contact with the tissue, could be expected because of chromium on the sixth oxidation stage Cr^{6+} that is the sensitizer in a small concentration and carcinogenic in the large quantities.
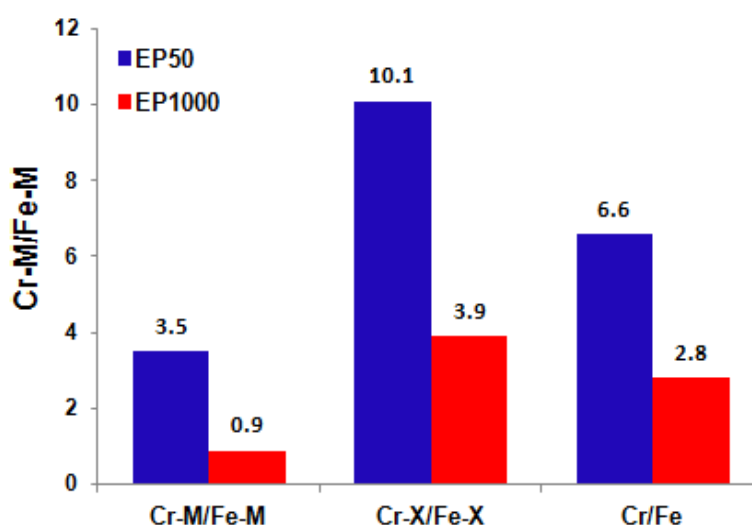

Fig. 6. Chromium metal to iron metal (Cr-M/Fe-M), chromium compounds to iron compounds (Cr-X/Fe-X) and total chromium to total iron (Cr/Fe) ratios as obtained on the basis of high-resolution XPS spectra

CONCLUSIONS

In that paper, the electropolishing at 50 A/dm^2 (EP50) and 1000 A/dm^2 (EP1000) in the non-standard electrolyte mixture (20 vol% H_3PO_4 and 80 vol% H_2SO_4), was described. On the basis of XPS data of the surface layers after both electrochemical treatments (EP50 and EP1000), a chromium to iron ratio (Cr/Fe) and chromium metal to iron metal (Cr-M/Fe-M) as well as chromium compounds to iron compounds (Cr-X/Fe-X) ratios, were found. After a standard EP50 the Cr-M/Fe-M, Cr-X/Fe-X, Cr/Fe ratios were over 3.8, 2.5, 2.3 times higher than those after the EP1000 treatment, respectively. For the presented part of the statistical plan (electrolyte composition: 20 vol% H_3PO_4 and 80 vol% H_2SO_4) the higher chromium enrichment after EP1000 treatment than that after EP50, was noted. The additional preliminary Authors' results have shown, that an opposite situation for other electrolyte, in which there was more H_3PO_4 than H_2SO_4, was observed.

ACKNOWLEDGMENTS

REFERENCES

1. Hryniewicz T.: Physicochemical and technological basics of electrolytic polishing of steels [in Polish], Monograph No 26, Publisher: Koszalin University of Technology, Koszalin 1989.

2. Rokosz K.: Electrochemical polishing of steels in the magnetic field [in Polish], Monograph No 219, Publisher: Koszalin University of Technology, Koszalin 2012, ISSN 0239-7129.

3. Hryniewicz T., Rokosz K., Rokicki R., Electrochemical and XPS Studies of AISI 316L Stainless Steel after Electropolishing in a Magnetic Field, Corrosion Science, 50(9), 2008, 2676-2681.

4. Rokosz K., Hryniewicz T., XPS measurements of LDX 2101 duplex steel surface after magneto-electropolishing, International Journal of Materials Research, 104(12), 2013, 1-10.

5. Rokosz K., Hryniewicz T., Raaen S., Cr/Fe ratio by XPS spectra of magnetoelectro-polished AISI 316L SS fitted by Gaussian-Lorentzian shape lines, Technical Gazette, 2014, 21(3), 533-538.

6. Hryniewicz T., Rokosz K., Investigation of selected surface properties of AISI 316L SS after magnetoelectropolishing, Materials Chemistry and Physics, 123, 2010, 47-55.

7. Rokicki R., US Patent No 7632390, http://www.patentgenius.com/patent/7632390.html

8. Hryniewicz T., Rokicki R., Rokosz K., Surface characterization of AISI 316L biomaterials obtained by electropolishing in a magnetic field, Surface & Coatings Technology, 202(9), 2008, 1668-1673.

9. Hryniewicz T., Rokicki R., Rokosz K., Corrosion Characteristics of Medical Grade AISI 316L Stainless Steel Surface after Electropolishing in a Magnetic Field, CORROSION (The Journal of Science and Engineering), Corrosion Science Section, 2008, 64(8), 660-665.

10. Hryniewicz T., Rokicki R., Rokosz K., Magnetoelectropolishing for metal surface modification, Transactions of the Institute of Metal Finishing, 85(6), 2007, 325-332.

11. Hryniewicz T., K. Rokosz K., Highlights of magnetoelectropolishing, Frontiers in Materials: Corrosion Research, 2014, 1(3), 1-7 (Inaugural Article); DOI: 10.3389/fmats.2014.00003.

12. Hryniewicz T., K. Rokosz K., Rokicki R., Magnetic Fields for Electropolishing Improvement: Materials and Systems, International Letters of Chemistry, Physics and Astronomy, 4 2014, 98-108.

13. Hryniewicz T., Concept of microsmoothing in electropolishing process, Surface and Coatings Technology, 1994, 64(2), 75-80.

14. Biesinger M.C., Payne B.P. , Grosvenor A. P., Lau L. W. M., Gerson A. R., Smart R. St. C., Resolving surface chemical states in XPS analysis of first row transmission metals, oxides and hydroxides: Cr, Mn, Fe, Co and Ni, Applied Surface Science, 2011, 257, 2717-2730.

15. Herrera-Gomez A., The Peak-Shirley Background (Shirley background in overlapping peaks), Centro de Investigación y de Estudios Avanzados del IPN Unidad Querétaro, Internal Report Created 8/2011, Last Update 2/2012.

16. Fairley N., http://www.casaxps.com, © Casa software Ltd., 2005.

17. CasaXPS Processing Software, CasaXPS Manual 2.3.15 Rev 1.0, Copyright © 2010 Casa Software Ltd, 19-20.

18. Walton J., Carrick A., The Casa Cookbook-The CasaXPS User's Manual, Part 1: Recipes for XPS data proceedings, 2009, ISBN: 9780954953300, Publisher: Acolyte Science.